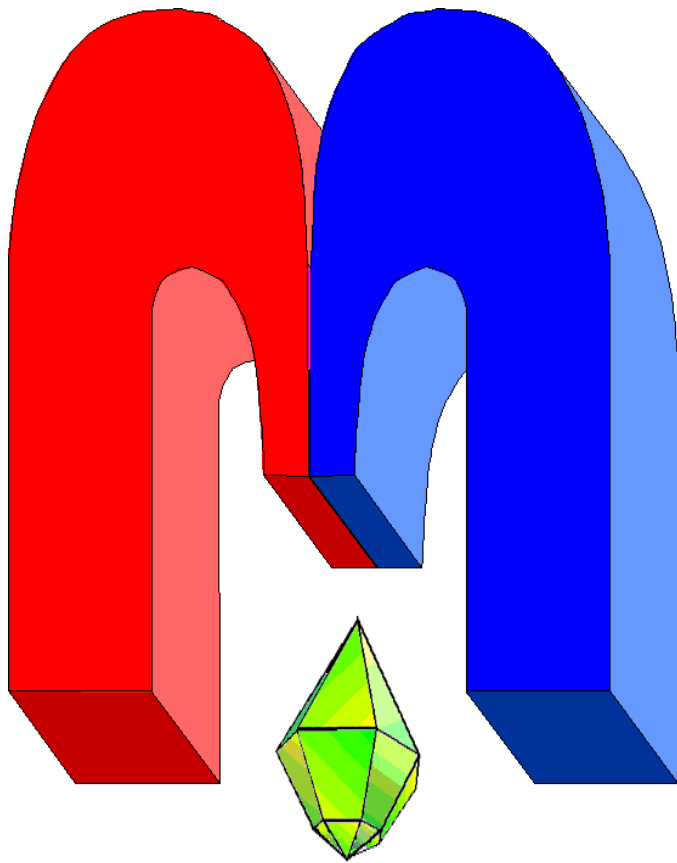


ISSN 2072-5981

doi: 10.26907/mrsej



***Magnetic  
Resonance  
in Solids***

Electronic Journal

*Volume 26*

*Issue 2*

*Article No 24204*

*1-9 pages*

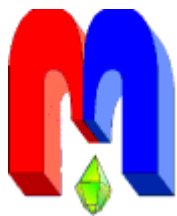
*June, 6*

*2024*

doi: 10.26907/mrsej-24204

<http://mrsej.kpfu.ru>

<https://mrsej.elpub.ru>



Established and published by Kazan University\*  
Endorsed by International Society of Magnetic Resonance (ISMAR)  
Registered by Russian Federation Committee on Press (#015140),  
August 2, 1996  
First Issue appeared on July 25, 1997

© Kazan Federal University (KFU)†

*"Magnetic Resonance in Solids. Electronic Journal" (MRSej)* is a peer-reviewed, all electronic journal, publishing articles which meet the highest standards of scientific quality in the field of basic research of a magnetic resonance in solids and related phenomena.

Indexed and abstracted by  
*Web of Science (ESCI, Clarivate Analytics, from 2015), Scopus (Elsevier, from 2012), RusIndexSC (eLibrary, from 2006), Google Scholar, DOAJ, ROAD, CyberLeninka (from 2006), SCImago Journal & Country Rank, etc.*

**Editor-in-Chief**

Boris **Kochelaev** (KFU, Kazan)

**Honorary Editors**

Jean **Jeener** (Universite Libre de Bruxelles, Brussels)

Raymond **Orbach** (University of California, Riverside)


**Executive Editor**

Yurii **Proshin** (KFU, Kazan)

[mrsej@kpfu.ru](mailto:mrsej@kpfu.ru)



This work is licensed under a [Creative Commons Attribution-ShareAlike 4.0 International License](https://creativecommons.org/licenses/by-sa/4.0/).

 This is an open access journal which means that all content is freely available without charge to the user or his/her institution. This is in accordance with the [BOAI definition of open access](https://www.boai.ru/).

**Technical Editors**

Maxim **Avdeev** (KFU, Kazan)

Vadim **Tumanov** (KFU, Kazan)

Fail **Sirae**v (KFU, Kazan)

**Editors**

Vadim **Atsarkin** (Institute of Radio Engineering and Electronics, Moscow)

Yurij **Bunkov** (CNRS, Grenoble)

Mikhail **Eremin** (KFU, Kazan)

David **Fushman** (University of Maryland, College Park)

Hugo **Keller** (University of Zürich, Zürich)

Yoshio **Kitaoka** (Osaka University, Osaka)

Boris **Malkin** (KFU, Kazan)

Alexander **Shengelaya** (Tbilisi State University, Tbilisi)

Jörg **Sichelschmidt** (Max Planck Institute for Chemical Physics of Solids, Dresden)

Haruhiko **Suzuki** (Kanazawa University, Kanazawa)

Murat **Tagirov** (KFU, Kazan)

Dmitrii **Tayurskii** (KFU, Kazan)

Valentine **Zhikharev** (KNRTU, Kazan)

**Invited Editor of Special Issue<sup>‡</sup>: Eduard Baibekov (KFU, Kazan)**

\* Address: "Magnetic Resonance in Solids. Electronic Journal", Kazan Federal University; Kremlevskaya str., 18; Kazan 420008, Russia

† In Kazan University the Electron Paramagnetic Resonance (EPR) was discovered by Zavoisky E.K. in 1944.

‡ Dedicated to Professor Boris Z. Malkin on the occasion of his 85th birthday

# Laser site selective spectroscopy of $\text{Er}^{3+}$ in $\text{ZnWO}_4$ single crystal

K.I. Gerasimov<sup>1,\*</sup>, M.M. Minnegaliev<sup>1</sup>, S.A. Moiseev<sup>1</sup>, K.A. Subbotin<sup>2</sup>, S.K. Pavlov<sup>2</sup>

<sup>1</sup>Kazan Quantum Center, Kazan National Research Technical University KAI,  
Kazan 420111, Russia

<sup>2</sup>Prokhorov General Physics Institute of the Russian Academy of Sciences,  
Moscow 119991, Russia

\*E-mail: [kigerasimov@mail.ru](mailto:kigerasimov@mail.ru)

(Received May 24, 2024; accepted May 30, 2024; published June 6, 2024)

The results of laser site selective and Zeeman spectroscopy studies of  $\text{ZnWO}_4$  single crystal doped with  $\text{Er}^{3+}$  ions are reported. Three types of  $\text{Er}^{3+}$  sites have been discovered. The energies of the levels of the  ${}^4\text{I}_{15/2}$  and  ${}^4\text{I}_{13/2}$  multiplets and the  $g$ -factors of several states were determined for three orientations of the crystal relative to the magnetic field. The possible structure of three types of sites and further research techniques are discussed.

**PACS:** 71.70.Ch, 75.10.Dg, 76.30.Kg, 71.70.Ej.

**Keywords:** rare-earth, site selective laser spectroscopy, optical Zeeman spectroscopy, crystal field levels,  $g$ -factors,  $\text{Er}^{3+}$ ,  $\text{ZnWO}_4$ .

*We heartily congratulate our dear teacher, highly experienced colleague, an outstanding physicist Professor B.Z. Malkin, on his anniversary. We wish you new great achievements, the same unquenchable thirst for learning new things and grateful followers.*

Sincerely yours, team of authors.

## 1. Introduction

Rare earth (RE) ions doped crystals are widely used in various fields of science and technology. Over the past two decades, quantum technologies (quantum computing, communications, sensors, etc.) have been intensively developing [1]. Due to the long coherence time of optical and microwave transitions, RE ions have become promising substances in the creation of basic devices of practical quantum information science, such as microwave and optical quantum memory [2], photonic qubit frequency converter [3], single-photon source [4], etc. For the successful implementation of a particular device, a large number of RE parameters in a particular crystal are important. These are, for example, the structure of energy levels,  $g$ -factors (for Kramers ions), dipole moments of transitions, the magnitude of inhomogeneous broadening on the transitions used, lifetimes of states and coherence times of optical, electronic and electron-nuclear transitions. To determine these parameters, the detailed spectroscopic studies are required, often involving high-resolution spectroscopy and coherent spectroscopy methods. From the point of view of achieving long coherence times required in the most part of quantum technologies, oxide crystals are considered as the most promising objects of the research. This is due to the high degree of dilution of the spin nuclear subsystem-reservoir of the host crystal and extremely low natural abundance (0.038%) of the oxygen isotope  ${}^{17}\text{O}$  having a nuclear spin ( $I = 5/2$ ). Over the past 10–15 years, the  $\text{Y}_2\text{SiO}_5$  orthosilicate crystal has remained the flagship in this direction. Here we can note the record coherence time of  $\text{Er}^{3+}$  and  $\text{Eu}^{3+}$  for electronic (4.4 ms [5], 2.6 ms [6]) and electron-nuclear (1.3 s [7], 6 hours [8]) transitions.

Many scientific groups are searching for new crystals with more suitable properties for specific quantum applications [9]. Recently we have studied  $\text{YPO}_4:\text{Er}^{3+}$  [10,11] and  $\text{CaMoO}_4:\text{Er}^{3+}$  [12] crystals, where relatively small inhomogeneous broadening of the optical lines (less than 200 MHz) and well-resolved hyperfine structure of several  $^4\text{I}_{15/2}(1) \rightarrow ^4\text{I}_{13/2}$  transitions of  $^{167}\text{Er}^{3+}$  ions were observed. In the recent studies of  $\text{CaWO}_4:\text{Er}^{3+}$  crystal, the dynamic properties of spin-orbit qubits have been investigated [13,14] and 23-ms coherence time on the  $\text{Er}^{3+}$  electron spin transition at 10 mK was achieved [15]. The  $\text{SrY}_2\text{O}_4:\text{Dy}^{3+}$  crystal is promising, in which a record value (1444 s) of the spin longitudinal relaxation time was found [16].

In this work, we present, for the first time of our knowledge, the investigations of  $\text{ZnWO}_4:\text{Er}^{3+}$  crystal using optical spectroscopy (including high-resolution and Zeeman spectroscopy) at helium temperatures. Room-temperature optical spectroscopy of  $\text{ZnWO}_4:\text{Er}^{3+}$  was previously reported in works [17,18] for the crystals grown by the Czochralski and the hydrothermal methods. From our point of view, the  $\text{ZnWO}_4:\text{Er}^{3+}$  crystal is promising for obtaining long coherence times in optical and microwave transitions due to the low concentration of ions having nuclear spin ( $^{17}\text{O} - 0.035\%$ ,  $^{183}\text{W} - 14.3\%$ ,  $^{67}\text{Zn} - 4.1\%$ ).

## 2. Experimental details and results

### 2.1. Crystal symmetry and crystal growth

$\text{ZnWO}_4$  crystal belongs to the family of monoclinic divalent-metal monotungstates  $\text{M}^{2+}\text{WO}_4$  (where  $\text{M} = \text{Mg}, \text{Zn}, \text{Cd}, \text{etc.}$ ). These compounds possess the so-called wolframite  $[(\text{Fe}, \text{Mn})\text{WO}_4]$  type with sp. gr.  $\text{P}2/\text{c} - \text{C}_{2h}^4$  [19]. Lattice parameters are 0.469263(5), 0.572129(7), 0.492805(5) nm for **a**, **b** and **c** axes respectively, and a  $\beta$  angle is  $90.6321(9)^\circ$  with two formula units per unit cell. Two representatives of this crystal family are magnesium monotungstate ( $\text{MgWO}_4$ , called huanzalaite in the natural mineral form) and zinc monotungstate ( $\text{ZnWO}_4$ , or sanmartinite). Trivalent erbium ions replace divalent zinc cations with a VI-fold oxygen coordination (site symmetry:  $\text{C}_2$ ) [20].

In order to prepare the charge for the  $\text{ZnWO}_4:\text{Er}$  crystal growth, the initial chemicals  $\text{ZnO}$ ,  $\text{WO}_3$  and  $\text{Er}_2\text{O}_3$  of the extra-pure grade were dried at  $600^\circ\text{C}$ , and then taken in the stoichiometric ratios. The concentration of  $\text{Er}^{3+}$  ions in the charge was 0.05 at.% in respect to  $\text{Zn}^{2+}$  amount. No any charge compensators of heterovalent  $\text{Zn}^{2+} \rightarrow \text{Er}^{3+}$  substitution were added. The required amounts of the chemicals were weighted with an Adventurer AX523 electronic analytical balance (OHAUS Corp., USA), and thoroughly mixed. The obtained mixtures were calcined at  $700^\circ\text{C}$  for 5 h in corundum crucibles at a muffle furnace to perform a solid phase synthesis of the compound. The  $\text{Er}:\text{ZnWO}_4$  single crystal was grown by the Czochralski technique at a “Kristall-2” growth setup (former USSR) in air from a Pt crucible. A single-crystalline bar cut from an undoped  $\text{ZnWO}_4$  perpendicular to **b** crystallographic axis was used as a seed. The pulling/rotation rates were 1 mm/h and 6 rpm, respectively. After finalizing the growth process and detaching the crystal from the melt, it was slowly (8 K/h) cooled down to room temperature in order to reduce the probability of the crystal cracking. The additional post-growth annealing of the grown crystal was performed in air at a muffle furnace for 15 days at  $900^\circ\text{C}$ . The heating and cooling rates were maintained at 10 K/h to avoid thermal shocks.

The obtained crystal was transparent, pale brownish-pink colored and did not contain cracks. The cross-section of the grown boule was strongly flattened along **b** crystallographic axis with well-developed natural faceting parallel to (010) crystallographic plane. This faceting has simplified the following orientation of the grown crystal in respect to its optical indicatrix axes. The actual  $\text{Er}^{3+}$  concentration in the crystal had not been measured. However, based on the data

from [21–23], one can predict the segregation coefficient of  $\text{Er}^{3+}$  between  $\text{ZnWO}_4$  crystal and the melt to be 0.15–0.2 without charge compensators. Therefore, the actual dopant concentration in our sample can be evaluated as 0.0075–0.01 at.% in respect to  $\text{Zn}^{2+}$  amount.

The crystal was cut in the shape of a parallelepiped with the sides of  $5.1 \times 4.5 \times 2.2$  mm, which corresponded to the directions of the  $\mathbf{b} \times \mathbf{N}_m \times \mathbf{N}_g$  axes with an accuracy of  $\pm 2$  degrees, where  $b$  is the crystallographic axis, and  $\mathbf{N}_m$  and  $\mathbf{N}_g$  are the optical indicatrix axes of the crystal. The  $\mathbf{b}$  axis coincides with the optical  $\mathbf{N}_p$  indicatrix.  $\mathbf{N}_m$  and  $\mathbf{N}_g$  lie in the  $\mathbf{a}$ – $\mathbf{c}$  plane and are rotated counterclockwise relative to  $\mathbf{a}$  and  $\mathbf{c}$  by 11.7 and 12.4 degrees, respectively [24, 25].

## 2.2. Optical and Zeeman spectroscopy

Sketch of the experimental setup for measurements of the luminescence, laser magneto-optical absorption spectra and luminescence decay is shown in Figure 1. The crystal was placed into a cryostation (Montana Instruments Corp.) with a magneto-optical module allowing measurements at magnetic fields up to 0.7 T. The sample was cooled to the temperatures of 4–30 K. High resolution absorption spectra were measured using continuous wave (CW) single-frequency diode laser (Toptica CTL 1500). The frequency of the laser emission was swept within 30 GHz. The sweep linearity and relative frequency accuracy of the laser emission were monitored using the transmission peaks of external temperature stable Fabry-Perot interferometer with free spectral range of 1 GHz and finesse of  $\sim 2000$ . Acousto-optical modulator (AOM) controlled the incident laser intensity. Transmitted light intensity was detected using APD110C/M avalanche photodiode (Thorlabs) and registered using digital oscilloscope - DPO7104C (Tektronix).

Luminescence spectra corresponding to  ${}^4\text{I}_{13/2} \rightarrow {}^4\text{I}_{15/2}$  transitions were measured using the monochromator (M833, SOLAR Laser Systems, reciprocal linear dispersion of  $\sim 1.5$  nm/mm) with CCD G9212-512S (Hamamatsu Photonics) detector. The same diode laser was tuned to the frequency of one of the  ${}^4\text{I}_{15/2}(1) \rightarrow {}^4\text{I}_{13/2}(1-5)$  transition excited the luminescence, where the number in brackets means the serial number of the level in the multiplet. AOM formed rectangular form of excitation pulses with duration of  $\sim 12$  ms. A mechanical chopper (Ch) blocked the input of the multimode fiber at the excitation duration to avoid strong illumination of the CCD. To measure the luminescence decay, an avalanche photodiode and an oscilloscope were used instead of a monochromator.

Three resonant transitions in the region of 1532–1535 nm were revealed as a result of measuring the absorption and luminescence spectra at a temperature of  $\sim 4$  K. Excitation at these transitions gave rise to different luminescence spectra with different decay times of luminescence. We believe that these transitions are associated with three different structurally nonequivalent erbium centers. The appearance of such centers is possible due to local and/or non-local compensation of the excess positive charge arising from hetero-valent substitution of divalent zinc by trivalent erbium. We designated these sites as **S1–S3** according to increasing energy of the resonant transition. The absorption linewidths of these transitions have different values. An example of a high-resolution absorption spectrum is shown in Figure 2. It should be emphasized that the resonant transitions of the **S1** and **S2** sites are located very close in frequency to each other (of  $\sim 11$  GHz) and the study of such sites requires methods of high spectral resolution ( $\Delta\lambda < 0.05$  nm).

Basic properties of  ${}^4\text{I}_{15/2}(1) \rightarrow {}^4\text{I}_{13/2}(1)$  absorption transitions and luminescence from  ${}^4\text{I}_{13/2}$  state of three types (**S1–S3**) of  $\text{Er}^{3+}$  centers in  $\text{ZnWO}_4$  crystal are summarized in Table 1. Despite the relatively large width of the absorption lines of **S1** and **S2** sites, the absorption coefficients have high values, from 3 to  $11 \text{ cm}^{-1}$ , depending on the direction of light propagation

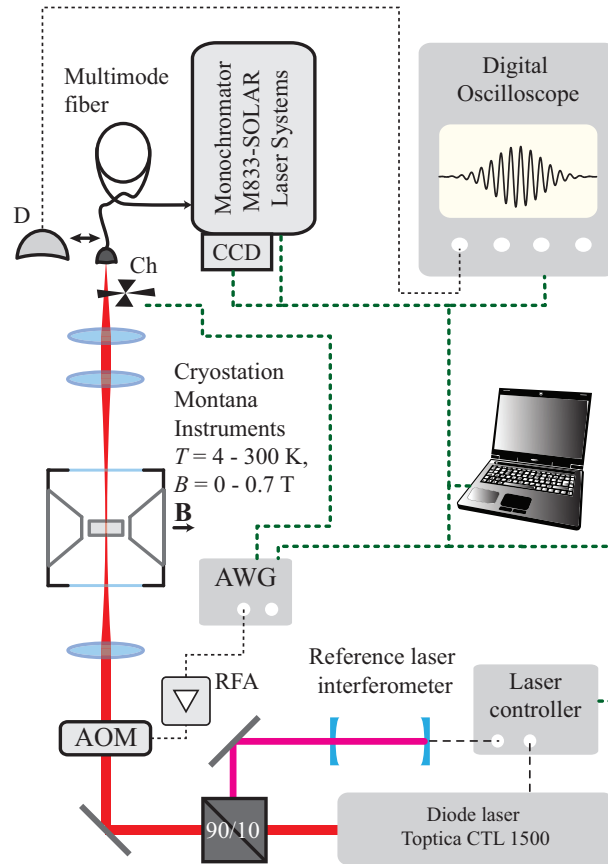


**Figure 1.** Sketch of experimental setup for absorption, luminescence, Zeeman spectra and luminescence decay measurement. D is an APD110C/M avalanche photodiode (Thorlabs), Ch - chopper, AOM - acousto-optical modulator, RFA - radiofrequency amplifier, AWG - arbitrary waveform generator, CCD - charge-coupled device, digital oscilloscope - DPO7104C (Tektronix).

and its polarization.

**Table 1.** Properties of  ${}^4I_{15/2}(1) \rightarrow {}^4I_{13/2}(1)$  absorption transitions and luminescence from  ${}^4I_{13/2}$  state of three types (**S1–S3**) of  $\text{Er}^{3+}$  centers in  $\text{ZnWO}_4$  crystal at the temperature of  $\sim 4\text{K}$ .  ${}^4I_{15/2}(1)$  denotes ground state,  ${}^4I_{13/2}(1)$  is the lowest Kramers doublet of  ${}^4I_{13/2}$  multiplet,  $\alpha$  is absorption coefficient

Site	<b>S1</b>	<b>S2</b>	<b>S3</b>
Wavelength, nm	1534.2	1534.1	1532.9
Wavenumber, $\text{cm}^{-1}$	6518.2	6518.6	6523.7
Linewidth, GHz	2.6	0.93	1.7
$\alpha$ ( $\mathbf{k} \parallel \mathbf{b}$ , $\mathbf{e} \parallel \mathbf{N}_g$ ), $\text{cm}^{-1}$	6	8	0.8
$\alpha$ ( $\mathbf{k} \parallel \mathbf{b}$ , $\mathbf{e} \parallel \mathbf{N}_m$ ), $\text{cm}^{-1}$	7.6	6.2	0.9
$\alpha$ ( $\mathbf{k} \parallel \mathbf{N}_g$ , $\mathbf{e} \parallel \mathbf{N}_m$ ), $\text{cm}^{-1}$	3	10.8	0.11
$\alpha$ ( $\mathbf{k} \parallel \mathbf{N}_g$ , $\mathbf{e} \parallel \mathbf{b}$ ), $\text{cm}^{-1}$	4.4	11.3	1
Luminescence time decay, ms	4.9	4.3	2.9

Example of luminescence spectra of sites **S1–S3** under selective excitation at transition frequencies corresponding to the  ${}^4I_{15/2}(1) \rightarrow {}^4I_{13/2}(1)$  transition and a temperature of  $\sim 8\text{K}$  is

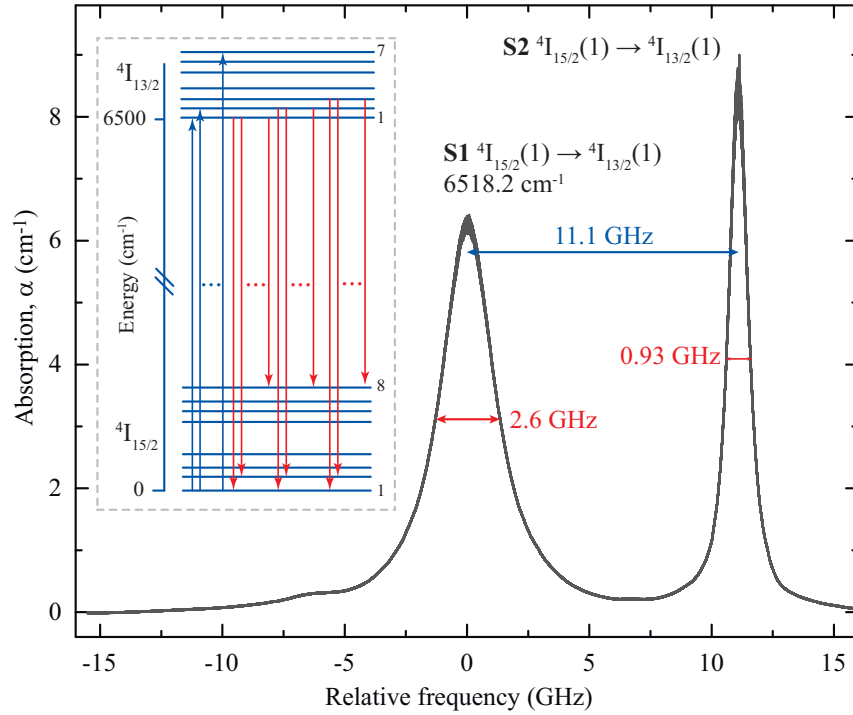


**Figure 2.** ZnWO<sub>4</sub>: Er<sup>3+</sup>  ${}^4I_{15/2}(1) \leftrightarrow {}^4I_{13/2}(1)$  resonant transition absorption lines of **S1** and **S2** sites at temperature of  $\sim 4$  K.  $\alpha$  is the absorption coefficient.  $\mathbf{e} \parallel \mathbf{N}_g$ ,  $\mathbf{k} \parallel \mathbf{b}$ . Frequency origin corresponds to center of  $6518.2 \text{ cm}^{-1}$  **S1** transition with frequency of  $195.411 \text{ THz}$  ( $\lambda \sim 1534.17 \text{ nm}$ ). A simplified scheme of absorption and luminescence transitions at temperature of  $\sim 8$  K is shown in the inset.

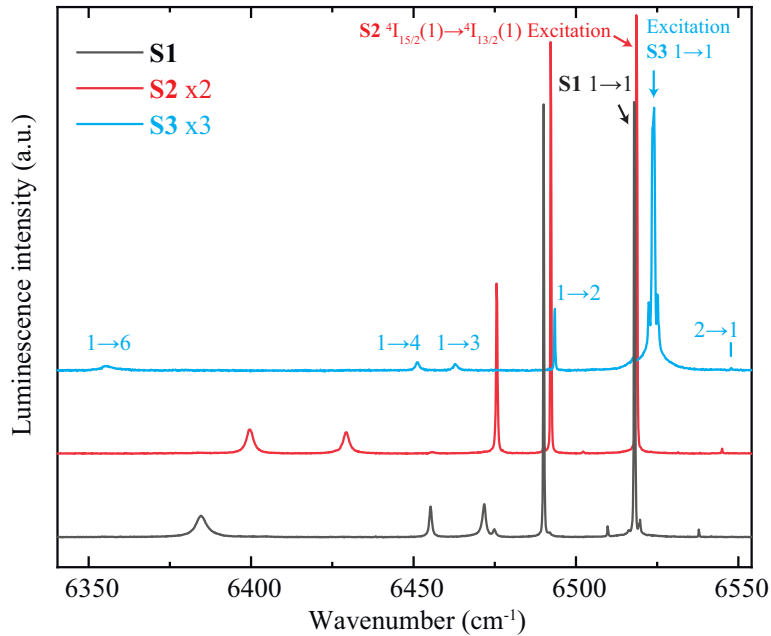


**Figure 3.** ZnWO<sub>4</sub>: Er<sup>3+</sup>  ${}^4I_{13/2}(1,2) \rightarrow {}^4I_{15/2}$  luminescence spectra of **S1**, **S2** and **S3** sites at  ${}^4I_{15/2}(1) \rightarrow {}^4I_{13/2}(1)$  transition excitation. Temperature is of  $\sim 8$  K. Spectra are shifted vertically for clarity. Excitation transitions are marked by arrows. The interpretation of luminescence lines with corresponding transitions is shown using the **S3** site as an example.

shown in the Figure 3. Weak lines associated with transitions from the  ${}^4I_{13/2}(2,3)$  states become observable in the luminescence spectra with increasing temperature. A small residual radiation

**Table 2.** Energies of levels (in  $\text{cm}^{-1}$ ) of  $\text{Er}^{3+}$  three sites in  $\text{ZnWO}_4$  single crystal measured by luminescence and absorption spectra

Site	<b>S1</b>	<b>S2</b>	<b>S3</b>
Energy and wavelength of excitation transition, $\text{cm}^{-1}$ (nm)	6518.2 (1534.2)	6518.6 (1534.1)	6523.7 (1532.9)
${}^4\text{I}_{13/2}$			
7	-	-	-
6	-	-	-
5	6572.7	-	-
4	6558.3	6557.6	-
3	6537.9	6545.2	6565.9
2	6530.3	6531.3	6547.7
1	6518.2	6518.6	6523.7
${}^4\text{I}_{15/2}$			
8	-	-	-
7	-	-	-
6	-	-	-
5	133.6	118.9	167.6
4	62.8	89.2	72.5
3	46.2	42.9	60.8
2	27.8	26.2	30.2
1	0	0	0

**Table 3.**  $g$ -factors of three Kramers doublets ( ${}^4\text{I}_{15/2}(1)$ ,  ${}^4\text{I}_{13/2}(1)$ ,  ${}^4\text{I}_{13/2}(3)$ ) of three types of  $\text{Er}^{3+}$  paramagnetic centers in three orientation of  $\text{ZnWO}_4$  crystal with regard to magnetic field  $\mathbf{B}$ .

Orientation of crystal	Transition	$g$ -factor level	<b>S1</b>	<b>S2</b>	<b>S3</b>
$\mathbf{B} \parallel \mathbf{N}_m, \mathbf{k} \parallel \mathbf{b}$	${}^4\text{I}_{15/2}(1) \rightarrow {}^4\text{I}_{13/2}(1)$	${}^4\text{I}_{15/2}(1)$	5.4	8.7	4.8
		${}^4\text{I}_{13/2}(1)$	4.8	8.2	3.9
	${}^4\text{I}_{15/2}(1) \rightarrow {}^4\text{I}_{13/2}(3)$	${}^4\text{I}_{15/2}(1)$	5.4	8.7	-
		${}^4\text{I}_{13/2}(3)$	3.3	3.7	-
$\mathbf{B} \parallel \mathbf{N}_g, \mathbf{k} \parallel \mathbf{b}$	${}^4\text{I}_{15/2}(1) \rightarrow {}^4\text{I}_{13/2}(1)$	${}^4\text{I}_{15/2}(1)$	5.2	7.6	4.7
		${}^4\text{I}_{13/2}(1)$	4.2	4.0	3.8
	${}^4\text{I}_{15/2}(1) \rightarrow {}^4\text{I}_{13/2}(3)$	${}^4\text{I}_{15/2}(1)$	5.1	7.6	-
		${}^4\text{I}_{13/2}(3)$	7.2	5.6	-
$\mathbf{B} \parallel \mathbf{b}, \mathbf{k} \parallel \mathbf{N}_g$	${}^4\text{I}_{15/2}(1) \rightarrow {}^4\text{I}_{13/2}(1)$	${}^4\text{I}_{15/2}(1)$	9.3	5.6	11.3
		${}^4\text{I}_{13/2}(1)$	7.1	5.0	9.6
	${}^4\text{I}_{15/2}(1) \rightarrow {}^4\text{I}_{13/2}(3)$	${}^4\text{I}_{15/2}(1)$	-	5.6	-
		${}^4\text{I}_{13/2}(3)$	-	3.0	-



from the pump laser was observed with the AOM turned off, so the intensities of the lines of resonant transitions do not have a true value.

The measured spectra made it possible to determine the energies of several levels in the  ${}^4I_{15/2}$  multiplet, see Table 2. Similar luminescence spectra of the **S1–S3** sites were observed at higher pump radiation frequencies. We interpreted these frequencies as the energy values of the 2–5 levels in the  ${}^4I_{13/2}$  multiplet, see Table 2. Some transitions, probably, have low probabilities and are not observed in the spectra. Therefore, the numbering of energy levels in the Table 2 corresponds to an increase in the energy of levels determined in the experiment and may not coincide with the actual level number in the multiplet.

Optical Zeeman spectroscopy of spectrally narrow absorption lines makes it possible to determine g-factors of two Kramers doublets if the selection rules allow all four possible transitions during doublet splitting in a magnetic field. In cases where this was true and the linewidths were less than  $\sim 5$  GHz, g-factors were measured for three crystal orientations in a magnetic field. Splitting and shifts of the optical transition frequencies were measured in the magnetic field varied from 0 to 0.6 T. From a linear fitting of these dependencies, we have calculated the values of the g-factors of  ${}^4I_{15/2}(1)$  ground doublet and one of two excited doublets ( ${}^4I_{13/2}(1)$  or  ${}^4I_{13/2}(3)$ ). The results are shown in the Table 3. Coincidence of g-factors for the ground doublet measured at  ${}^4I_{15/2}(1) \rightarrow {}^4I_{13/2}(1)$  and  ${}^4I_{15/2}(1) \rightarrow {}^4I_{13/2}(3)$  transitions indicates that the  ${}^4I_{15/2}(1) \rightarrow {}^4I_{13/2}(3)$  transition indeed belongs to the selected center, which is in agreement with the results of site selective laser spectroscopy.

### 3. Conclusions and Outlook

ZnWO<sub>4</sub> single crystal doped with Er<sup>3+</sup> ions was investigated by site selective laser and Zeeman spectroscopy. Three types of Er sites (paramagnetic centers) were observed and investigated for the first time of our knowledge. For sites **S1** and **S2**, relatively high values of g-factors (9.3 and 8.7 for orientations  $\mathbf{B} \parallel \mathbf{b}$ ,  $\mathbf{k} \parallel \mathbf{N}_g$  and  $\mathbf{B} \parallel \mathbf{N}_m$ ,  $\mathbf{k} \parallel \mathbf{b}$ , respectively) and energy values of the first excited doublet  ${}^4I_{15/2}(2)$  were obtained (for example, compared to Er in YPO<sub>4</sub> [11] or CaMoO<sub>4</sub> [12] crystals). This can lead to higher values of the longitudinal spin relaxation times of the ground Kramers doublet and have a positive effect on increasing the coherence times of spin and optical transitions. Giant values of absorption coefficients (for example, 11 cm<sup>-1</sup> for the **S2** site) will make it possible to reduce the Er concentration by an order of magnitude and weaken the dipole-dipole interactions of Er ions. These properties can provide significantly suppress the relaxation processes and allows us to hope the crystal can be successfully used in the practical quantum technologies. To establish the nature of the discovered three sites, the studies using electron paramagnetic resonance (EPR) and double electron-nuclear resonance (ENDOR) methods are required, which we plan in the future. The g-factors of the ground Kramers doublets measured in this work will make it possible to correlate the results of optical spectroscopy with the structure of sites obtained from EPR and ENDOR future data.

### Acknowledgments

K.I.G., M.M.M. and S.A.M. acknowledge support from the Ministry of Education and Science of Russia, Reg. No. NIOKTR 121020400113-1. The research activity of the team from Prokhorov General Physics Institute of the Russian Academy of Sciences has been supported by Russian Scientific Fund (grant No 23-22-00416)

## References

1. Thiel C., Böttger T., Cone R., *J. Lumin.* **131**, 353 (2011).
2. Guo M., Liu S., Sun W., Ren M., Wang F., Zhong M., *Front. Phys.* **18**, 21303 (2023).
3. Han X., Fu W., Zou C.-L., Jiang L., Tang H. X., *Optica* **8**, 1050 (2021).
4. Ourari S., Dusanowski L., Horvath S. P., Uysal M. T., Phenicie C. M., Stevenson P., Raha M., Chen S., Cava R. J., de Leon N. P., Thompson J. D., *Nature* **620**, 977 (2023).
5. Böttger T., Thiel C. W., Cone R. L., Sun Y., *Phys. Rev. B* **79**, 115104 (2009).
6. Equall R. W., Sun Y., Cone R. L., Macfarlane R. M., *Phys. Rev. Lett.* **72**, 2179 (1994).
7. Rančić M., Hedges M. P., Ahlefeldt R. L., Sellars M. J., *Nature Phys.* **14**, 50 (2018).
8. Zhong M., Hedges M. P., Ahlefeldt R. L., Bartholomew J. G., Beavan S. E., Wittig S. M., Longdell J. J., Sellars M. J., *Nature* **517**, 177 (2015).
9. Campbell G. T., Ferguson K. R., Sellars M. J., Buchler B. C., Lam P. K., in *Quantum Inf.* (Wiley, 2016) pp. 723–740.
10. Popova M. N., Klimin S. A., Moiseev S. A., Gerasimov K. I., Minnegaliev M. M., Baibekov E. I., Shakurov G. S., Bettinelli M., Chou M. C., *Phys. Rev. B* **99**, 235151 (2019).
11. Gerasimov K. I., Sabirov T. N., Moiseev S. A., Baibekov E. I., Bettinelli M., Chou M., Yen Y.-C., Popova M., *Opt. Spectrosc.* **131**, 607 (2023).
12. Gerasimov K., Baibekov E., Minnegaliev M., Shakurov G., Zaripov R., Moiseev S., Lebedev A., Malkin B., *J. Lumin.* **270**, 120564 (2024).
13. Bertaina S., Gambarelli S., Tkachuk A., Kurkin I. N., Malkin B., Stepanov A., Barbara B., *Nature Nanotech.* **2**, 39 (2007).
14. Bertaina S., Shim J. H., Gambarelli S., Malkin B. Z., Barbara B., *Phys. Rev. Lett.* **103**, 226402 (2009).
15. Le Dantec M., Rančić M., Lin S., Billaud E., Ranjan V., Flanigan D., Bertaina S., Chanelière T., Goldner P., Erb A., Liu R. B., Estève D., Vion D., Flurin E., Bertet P., *Sci. Adv.* **7**, eabj9786 (2021).
16. Malkin B. Z., Yusupov R. V., Gilmutdinov I. F., Batulin R. G., Kiiamov A. G., Gabbasov B. F., Nikitin S. I., Barbara B., *Phys. Rev. B* **109**, 054434 (2024).
17. Yang F., Tu C., Li J., Jia G., Wang H., Wei Y., You Z., Zhu Z., Wang Y., Lu X., *J. Lumin.* **126**, 623 (2007).
18. Minh N. V., Hung N. M., Xuan Thao D. T., Roeffaers M., Hofkens J., *J. Spectrosc.* **1**, 4 (2013).
19. Kravchenko V. B., *J. Struct. Chem.* **10**, 139 (1969).
20. Schofield P. F., Knight K. S., Cressey G., *J. Material. Science* **31**, 2873 (1996).

21. Subbotin K. A., Titov A. I., Pavlov S. K., Volkov P. A., Sanina V. V., Lis D. A., Lis O. N., Zimina Y. I., Didenko Y. S., Zharikov E. V., *J. Cryst. Growth* **582**, 126498 (2022).
22. Yang F., *J. Mater. Res.* **27**, 2096 (2012).
23. Yang F., Tu C., *J. Alloys Comp.* **535**, 83 (2012).
24. Wang H., Lin Y., Zhou Y.-D., Chen G., Zhou T., Wang J., Hu B.-Q., *Acta Physica Sinica* **38**, 670 (1989).
25. Volokitina A., David S. P., Loiko P., Subbotin K., Titov A., Lis D., Solé R. M., Jambunathan V., Lucianetti A., Mocek T., Camy P., Chen W., Griebner U., Petrov V., Aguiló M., Díaz F., Mateos X., *J. Lumin.* **231**, 117811 (2021).